Int J Syst Assur Eng Manag (December 2023) 14(6):2605–2625
https://doi.org/10.1007/s13198-023-02124-7

ORIGINAL ARTICLE

Design and simulation of six-phase UPFC power quality enhancement with improved GWO based decoupled power control strategy

Srinivas Nakka[1] · R. Brinda[1] · T. Sairama[2]

Received: 20 March 2023 / Revised: 31 July 2023 / Accepted: 24 August 2023 / Published online: 17 September 2023

Abstract The unified power flow controller (UPFC) is a device used in power systems to control and optimize the flow of electric power. It is a flexible AC transmission system device that combines several power electronic components to provide comprehensive control over voltage, active power, and reactive power in transmission lines. This research offers an improved gray wolf optimization (IGWO)-based decoupled power control strategy (DPCS) for a six-phase UPFC (6P-UPFC) to enhance power quality. The proposed 6P-UPFC-DPCS divides its control efforts between reactive power control and active power control. This is because the UPFC can independently regulate the transmission line's voltage and phase angle by decoupling the active and reactive power flows. A fault isolation technique is provided for isolating the damaged part of the transmission line, which would increase system efficiency and dependability. By analyzing the voltage and current signals at the UPFC terminals, as well as the line impedance, it is possible to ascertain whether a problem exists. After the trouble spot has been identified, the 6P-UPFC must be adjusted to compensate for the predicted impedance of the damaged line to restore power to the system. After that, the coordinated voltage and current are managed through the virtual impedance. The PI controller's proportional and integral gains, as well as the inverter's voltage phase angle and magnitude, are optimized using the IGWO method. The performance and dependability of the control strategy are further enhanced by tuning the controller parameters for the 6P-UPFC-DPCS controller using an IGWO approach. The simulation results show that the proposed 6P-UPFC-DPCS might reduce the false setting time to 0.01 s, boost the power factor to 0.98, and lower the total harmonic distortion to 1.40%.

Keywords Decoupled power control strategy · Six-phase unified power flow controller · Improved grey wolf optimization · Total harmonic distortion

Abbreviations

UPFC	Unified power flow controller
FACTS	Flexible AC transmission system
IGWO	Improved gray wolf optimization
6P-UPFC	Six-phase UPFC
DPCS	Decoupled power control strategy
FST	False setting time
THD	Total harmonic distortion
VSI	Voltage source inverters
MOC	Multi-objective control
IPC	Indirect power control
MPC	Model predictive control
FLC	Fuzzy logic controller
GA	Genetic algorithm
PSO	Particle swarm optimization
VSC	Voltage source converter
TBS	Thyristor bypass switch
BBR	Buck–boost rectifier
RMS	Root mean square
DSTATCOM	Distributive static synchronous compensator

✉ Srinivas Nakka
nakkasrinu@gmail.com

R. Brinda
rbrinda7971@yahoo.co.in

T. Sairama
tsairama@yahoo.co.in

[1] Department of Electrical Engineering, Annamalai University, Chidambaram, India

[2] Department of Electrical and Electronics Engineering, Vardhaman College of Engineering, Hyderabad, Telangana, India

1 Introduction

The 6P-UPFC is a kind of FACT (Smith 2023) that is utilized in power systems to manage the flow of energy and improve power quality. As compared to the tried-and-true UPFC (Chen et al. 2018), which operates on a 3-phase power system, the 6P-UPFC is an upgrade. Two parallel-connected three-phase voltage source inverters (VSI) (Elsaharty et al. 2018) make up the 6P-UPFC. The two VSIs may talk to one another and exchange information via a mutual DC bus if they are attached to one another using direct current. The 6P-UPFC uses two sets of three-phase ac voltages that are rotated by 30 degrees to mimic the six phases. Each of the six phases' voltage and phase angle was modified independently by the two VSIs. The 6P-UPFC is superior to the traditional UPFC in many significant ways. Unlike a standard UPFC, which can only regulate power flow in three phases, the 6P-UPFC can do it in all six. Because of this, the 6P-UPFC can easily adapt to the needs of the present power grid, which typically makes use of six-phase transmission lines. Moreover, the 6P-UPFC may improve power quality by reducing voltage fluctuations and harmonic distortion (Taheri et al. 2018). Several control mechanisms for the 6P-problematic UPFC's regulation have been reported in the scientific literature. The DPCS is favored because of its flexibility in regulating active and reactive power flows throughout all six phases. This method improves the system's adaptability and manageability by allowing for phase-by-phase control of power flow. The 6P-UPFC is promising for the future of electric power since it has the possibility to develop the stability, reliability, and efficiency of the power system (Shotorbani et al. 2018). Nevertheless, further research is needed to hone the control methods and evaluate the 6P-efficacy of UPFCs in a variety of settings. 6P-UPFC can regulate power flow in the system using a variety of power control approaches (Zhang et al. 2018).

Some of the more common methods are DPCS, indirect power control (IPC), multi-objective control (MOC), control based on an adaptive neuro-fuzzy inference system (ANFIS), control based on backstepping (BSC), and model predictive control (MPC). The DPCS (Miotto et al. 2018) is a method of control that has an immediate effect on the active and reactive power flows. The regulation is based on the deviation between the target and actual values. The DPCS is a simple and effective method of control that is distinguished by its fast dynamic reactivity and high transient stability. The IPC (Nouri et al. 2018) is a technique for adjusting the system's active and reactive power flow by manipulating the voltage and its phase angle. IPC uses the discrepancy between the reference voltage and the measured voltage as its error metric. Input–output control has high efficiency in the steady state and a high degree of dependability. Due to this, DPCS (Kumar and Chakravarthy 2018) is a type of control that splits the active and reactive power flows over six phases. The DPCS allows for phase-by-phase power regulation, which improves the system's responsiveness and degree of controllability. Further, MOC (Tamimi and Cañizares 2018) is a control strategy that simultaneously improves voltage stability, reduces active power losses, and reduces harmonic distortion. The intricacy of MOC necessitates the use of sophisticated optimization algorithms and state-of-the-art modeling techniques. In addition, ANFIS (Qi et al. 2018), a technique of control that uses a fuzzy logic controller (FLC) (Bone et al. 2018) and a neural network (Biswal et al. 2018), was used to optimize the 6P-UPFCs. So, ANFIS can learn the system's behavior and adapt to changing operating conditions, which improves the robustness and adaptability of the system. Additionally, the 6P-UPFCs was optimized with the help of a predictive model of the system using a control approach called MPC (Zhu et al. 2018). This model is used to create a simulation of the system. The MPCcan predict how the system will behave in the future and alter the control inputs to achieve your goals. Due to MPC's complexity, advanced modeling and optimization tools are necessary for its implementation. Two decoupling control signals was used to divide the BSC (Fang, et al. 2018) system into two independent backstepping controllers. This allows each user to set their own preferences for the controller's settings. This means that it is possible to reduce overall harmonic distortion while maintaining a steady DC bus output voltage and a sinusoidal input current.

The motivation behind the research is to enhance power system performance and efficiency by developing an improved control strategy for the UPFC. By utilizing the proposed DPCS and the optimization capabilities of the IGWO algorithm, the aim is to improve power quality, minimize losses, and enhance system stability. Additionally, the introduction of a fault isolation technique addresses the need for efficient fault detection and restoration, contributing to increased dependability and overall performance of the power system.Short-term adjustments to active and reactive capacities may also be made incidentally. Resilience was constructed against the filter's inductance, power grid oscillations, and load variations. These are some of the commonly used power control strategies for 6P-UPFC. The selection of the control strategy depends on the specific application, the system requirements, and the available resources.The challenge of improving the power quality of the power system has a comprehensive solution in the form of the IGWO algorithm, the fault isolation technique, and the coordination strategy described for the 6P-UPFC system. There is potential for the proposed technique to provide significant results for power corporations if implemented in the real world.The novel contributions of the works are as follows:

- Development of an IGWO-based DPCS for 6P-UPFC is a novel control strategy that utilizes the IGWO algorithm to optimize the performance of the 6P-UPFC, enhancing its power control capabilities.
- The proposed 6P-UPFC-DPCS aims to improve power quality by independently regulating voltage and phase angle, enabling efficient control overactive and reactive power flows. This contributes to minimizing power losses and maximizing system efficiency.
- The research introduces a fault isolation technique for identifying and isolating damaged parts of the transmission line. By analyzing voltage and current signals at the UPFC terminals and line impedance, the system can identify problematic areas, allowing for timely corrective actions.
- The IGWO algorithm is employed to optimize the control parameters of the 6P-UPFC-DPCS, including the proportional and integral gains of the PI controller, as well as the voltage phase angle and magnitude of the inverter. This optimization process contributes to improving the overall performance and dependability of the control strategy.

The rest of the article is organized as follows: Sect. 2 covers the various existing UPFC controlling methods, which focused on literature surveys. Section 3 focused on the implementation and mathematical analysis of the proposed 6P-UPFC-DPCS with IGWO optimization. Section 4 focused on results and discussion. Finally, Sect. 5 concludes the article with future possibilities.

2 Literature survey

2.1 Survey on basic UPFC control techniques

Although significant work has gone into simulating and designing UPFC control techniques for power flow management, there has been a dearth of investigational certification of various UPFC controllers and their performance in real-time operation. To solve the issues with traditional UPFCs, Albatsh et al. (2017) presented a FLC, to dynamically regulate power flow over transmission lines. Reactive power control in power networks with ample renewable resources is the subject of a comprehensive literature analysis by Sarkar et al. (2018). The reactive power requirements of REGs are totaled across several grid codes to see whether they meet the needs of the future network. A strategy for regulating the optimally acquired component of current sharing was suggested by Elamari et al. (2019). This data is being added to a database for future reference. By using proportional resonant controllers and sinusoidal pulse width modulation, theycan provide the ideal inductive and capacitive branch currents for the UPFCs, which are subsequently transformed into gating signals for the voltage source converter (VSC) using Park's law. It is done so that a UPFC can provide excellent inductive and capacitive branch currents. Rahman et al. (2020) discuss control schemes for series and shunt converters to regulate the load voltages of the distribution feeder while simultaneously lowering the 2HV term on the UPFC's dc-link. Management like this is discussed in Haque et al. (2020). Reducing the 2 HV term on the DC-link necessitates adjustments to the negative sequence current of the shunt converter. With the use of distribution static synchronous compensator (DSTATCOM) for reactive power adjustment, Hamdan et al. (2020) suggest that the fault ride-through capabilities and dynamic performance of a grid-connected PV/wind hybrid power system was improved. The purpose of this change was to increase the system's ability to recover quickly from errors. Accurate modeling of the monitor system and power electronics of the 72-pulse VSC-based GUPFC is presented in the work of Abasi et al. (2020), who aim to aid in meeting operating limits and improving power quality by lowering harmonic levels. The proposed paradigm rules out the use of active or passive filters to reduce harmonic content in the GUPFC.

2.2 Survey on advanced control strategies for UPFC

Kamel et al. (2015) incorporatedboth power and current injections in their report using a C-UPFC model. A modified Newton–Raphson method, based on combined mismatches in load flow, now incorporates the newly created model. Periodically, the parameters of the shunt UPFCs and the series voltage controllers are tweaked. According to research by Hassan et al. (2013), a UPFCwas utilized in conjunction with a genetic algorithm (GA) to stabilize many power systems simultaneously. The GA is used to determine the optimal placement for the UPFC and to calibrate its controller factors for a wide range of possible operational conditions. For the distribution network, Yuan et al. (2022) proposed a novel multiline rapid electromagnetic UPFC, which has compact construction, great economy, fast response, and high reliability in the conventional regulating mode. Parvathy et al. (2015) devised a standard PI controller-based decoupled control technique for shunt and series converters to follow reference work power inputs. This system was meant to regulate the converters. Makvandi et al. (2021) used wide-area signals to create a one-of-a-kind supplemental neuro-controller architecture for UPFCs. Dual heuristic programming is an adaptive critique procedure that formed the basis of the new design. The suggested controller would improve power system reliability by injecting extra signals into the UPFC series inverter. Monteiro et al. (2014) provide a concept for three-phase matrix converters that function as

UPFCs by contrasting the presentation of decoupled, linear, and direct-power-conversion systems.

2.3 Survey on optimization techniques and applications for UPFC

Parvathy et al. (2020) created a non-linear state-space model of UPFC. This model considers not only the effects of source impedance but also the transfer of energy in the passive components and the voltage functions at the VSC output. The UPFC's non-linear model is controlled by a non-linear controller, and so on and so forth. Yu et al. (2021) propose a series-shunt combined power converter architecture to equally distribute power throughout the power grid to maximize operational stability and transmission capacity. If this setup is connected to a weak grid, it was used to regulate power flows inside the system. Active power decoupling and smooth mode switching are both possible in a bidirectional single-phase ac/dc converter, as shown by Wang et al. (2022). It has been shown that power decoupling methods are helpful in reducing the size of the generally huge dc bus electrolytic capacitors seen in single-phase low-power level converter systems. Yet, in a significantly reduced E-caps situation, such as when dealing with transient events like quick bidirectional switching or sudden load changes, it has been shown that the whole system was brittle and unstable. The reason for this is that the present demand exceeds the available e-capacity. In their study, Yan et al. (2021) investigate a wide variety of DPCS approaches for three-phase, two-level PWM converters.

2.4 Survey on advanced techniques and modeling for UPFC

The power formula for PWM rectifiers is briefly explained in the first section of this article. Afterwards, the paper delves into the nuts and bolts of the conventional table-based method and the subsequent enhancements to it. Yang et al. (2019) investigated the UPFC system-level control approach to enhance the transfer capacity and voltage regulation of regional power grids. After explaining the fundamentals of converter-level control, a comparable UPFC model is offered. It was proposed by Yu et al. (2008) that a quadratic model be used for both power flow and optimal reactive power flowto better understand the dynamics of power conversion from AC to DC. The magnitudes of the voltages on both sides of a perfect converter transformer are included as additional state variables when constructing quadratic models. When equality constraints are present, the role of converter controls is analyzed. In addition, the well-established quadratic expression of UPFC is included in the proposed models. For direct power regulation of a three-phase voltage-source PWM rectifier, Wai et al. (2019) settled on the BSC configuration. The power factor of this three-phase rectifier was adjusted by changing the dc output voltage and the instantaneous reactive power.

2.5 Survey on contributions in other fields

In Singh (2022), the authors focused on studying the impact of quarantine measures on the dynamics of the COVID-19 pandemic. The authors use a fractional-order dynamical model to analyze the effects of different quarantine strategies on the spread and control of the virus. In Ong et al. (2022), the authors compare the performance of pre-trained and convolutional neural networks (CNNs) for classifying different species. In Mahajan et al. (2022a), the authors proposed an image segmentation approach that combines the adaptive flower pollination algorithm with type II fuzzy entropy. The authors aim to enhance the accuracy and efficiency of image segmentation by incorporating the advantages of both algorithms. The authors present an image-based automatic segmentation method for leaf analysis using a clustering algorithm. The study focuses on accurately segmenting leaf images to extract meaningful features for various applications, such as plant disease detection and classification. In Sharma et al. (2022), the authors introduced a hybrid method for feature selection that combines signal processing and complex algebra techniques. The authors aim to improve feature selection accuracy and efficiency by leveraging the advantages of both domains. In Mahajan and Pandit (2021), the authors proposed a hybrid optimization approach by combining the Aquila optimizer with the arithmetic optimization algorithm. The study focuses on solving global optimization tasks efficiently and accurately. In Mahajan et al. (2022b), the authors provided insights into image segmentation techniques and their connection to optimization methods. The authors discuss the importance of image segmentation in various applications and provide a brief overview of optimization techniques used in image segmentation. In Mahajan and Oandit (2022), the authors propose a fusion approach that combines multiple modern meta-heuristic optimization methods using the arithmetic optimization algorithm. The goal is to improve the performance and convergence speed of global optimization tasks. The proposed fusion approach is compared with individual optimization methods using benchmark functions, demonstrating its effectiveness in achieving better optimization results. In Mahajan et al. (2022c), the authors introduced a hybrid optimization algorithm that combines the arithmetic optimization algorithm with the Hunger Games search technique for global optimization. In Mahajan et al. (2022d), the authors aim to enhance the exploration and exploitation capabilities of the algorithm to achieve better optimization results. The hybrid approach is evaluated using various benchmark functions, showcasing its effectiveness in finding optimal solutions.

In Tiwari et al. (2018) authors focused on voltage stability analysis in power systems using a hybrid controller. The authors propose a novel approach that combines shunt and series combinations of FACTS devices. The paper discusses the design and implementation of the hybrid controller and presents a voltage stability analysis using this approach. In Sengupta et al. (2018) authors the authors address transient stability enhancement in a hybrid wind-photovoltaicfarm by incorporating a DSTATCOM. The paper discusses the design and integration of the DSTATCOM in the hybrid farm and evaluates its impact on transient stability. In Yadav et al. (2020) authors propose a hybrid controller that combines different power flow control devices. The paper presents the design and implementation of the hybrid power flow controller and evaluates its effectiveness in enhancing transient stability. In Tiwari and Kumar (2023) authors provided an overview and bibliographic analysis of particle swarm optimization (PSO) applications in electrical power systems. The authors discuss the concepts and variants of PSO and present advances in its application in power system optimization. The paper explores the use of PSO in various power system domains and provides insights into its effectiveness.

3 Proposed methodology

The FACTS family includes the UPFC, a device that can control the voltage and current profiles of a power grid. Six-phase power electronics allow for more precise regulation than the traditional three-phase UPFC. This advancement has led to the development of a newer design known as the 6P-UPFC. Figure 1 depicts the proposed block design of a single line diagram for a power system using 6P-UPFC. This simulation represents a transmission line that is 60 km in length, operates at a frequency of 60 Hz, and has six phases supplying power to a load at the other end. The six phases of the alternating current source must be rotated by sixty degrees with respect to one another. As a six-phase ac supply is not readily available, we must make do with two three-phase ac generators. The letters A, C, and E stand for the three activities taken by Source 1, whereas the letters B, D, and F stand for the three actions taken by Source 2. A reference phase "A" from source 1 is used to shift the reference phase "B" from source 2 by the same amount with respect to phase "A" resulting in a phase difference of 60 degrees. The six-phase transmission line is being simulated using a simulation built on the distributed parameter model.

Figure 2 shows the proposed 6P-UPFC-DPCS-IGWO block diagram. Measure the real and reactive power flows in the six-phase transmission line. Detect faults in the six-phase transmission line using the fault detection unit.Initialize the DPCS-IGWO algorithm with the objective function as the total power loss in the system. Generate an initial population of grey wolves and evaluate their fitness based on the objective function. Iterate the DPCS-IGWO algorithm until convergence criteria are met. Within each iteration, update the position of each grey wolf based on its hunting behavior. Calculate the fitness of each new place of the grey wolves. Update the best position and the worst position of the grey wolves. Calculate the new position of the grey wolves using the best, worst, and average positions. Signals for the UPFC with 6P control was computed using the GWO-optimized parameters. The 6P-UPFC can regulate the active and reactive power flows in the transmission line in response to the command signals. In this case, a DPCS is in charge, and it controls the 6P-UPFC by keeping active and reactive power regulation distinct.

The DPCS for 6P-UPFC consists of two separate control loops, one for active power flow and one for reactive power flow. The active power control loop alters the phase angle between the injected three-phase AC voltage components from the UPFC, whereas reactive power control loop modifies the injected voltage components' amplitude. In

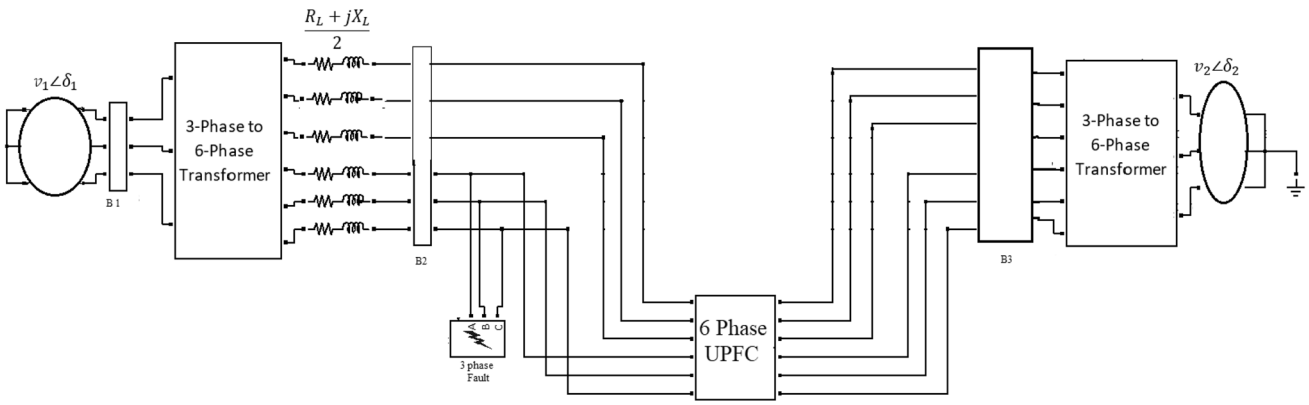

Fig. 1 Single line diagram of 6P-UPFC based power system

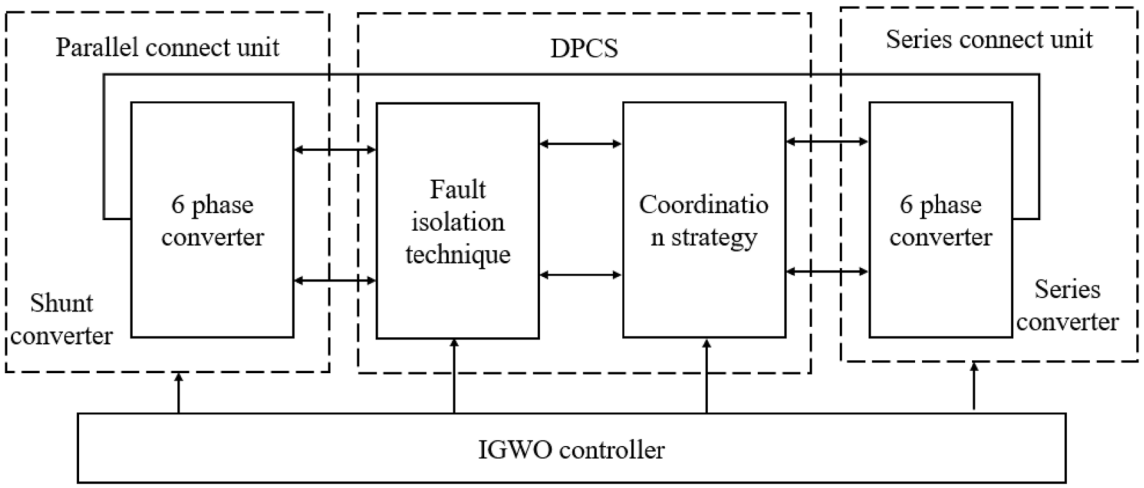

Fig. 2 Proposed 6P-UPFC-DPCS-IGWO block diagram

mathematics, the active power control loop is represented by the equation:

$$\frac{d\delta}{dt} = K_p\left(P_m - P_e\right) - K_i * \delta \tag{1}$$

In this case, δ denotes the phase angle between the two different sets of voltage components; P_m represents the active power flow that was really measured; P_e is the active power flow that was requested; K_p represents the proportional gain; and K_i denotes the integral gain. In a similar fashion, the equation that was used to express the reactive power control loop is as follows:

$$\frac{dVq}{dt} = K_p\left(Q_m - Q_e\right) - K_i * V_q \tag{2}$$

here V_q is the reactive voltage component injected by the UPFC, Q_m is the measured reactive power flow, Q_e is the desired reactive power flow, K_p is the proportional gain, and K_i is the integral gain. To better regulate the power flow and voltage profile of a power system, the DPCS for 6P-UPFC separates the control of active and reactive power flow. However, it requires more complex control algorithms and hardware than traditional three-phase UPFCs, which can make implementation more challenging. The performance of this DPCS is optimized by IGWO. If a fault is detected in the transmission line, activate the fault isolation and coordination strategy. Determine the location and type of fault using the fault detection unit. Generate signals for fault isolation and coordination strategy based on the location and type of fault. Apply the fault isolation and coordination strategy signals to the transmission line to isolate the fault and maintain power supply to healthy parts of the system. Repeat the process to continuously monitor and regulate the real and reactive power flows in the six-phase transmission line.

3.1 DPCS

Separate control loops are used in the DPCS for power electronic devices like the 6P-UPFC to regulate the active and reactive power flows, respectively. It's helpful for controlling power flow in a power system since it provides for separate management of active and reactive power. The mathematical analysis of the DPCS can be described using the following equations:

3.1.1 Active power control

The active power control loop involves controlling the active power flow using the d-axis current components of the two VSC. The control equation for the active power flow is given by:

$$P_{ref} = P_{set} - K_p * \left(Id1_{ref} - Id1\right) - K_p * \left(Id2_{ref} - Id2\right) \tag{3}$$

where P_{ref} is the desired active power flow, P_{set} is the actual power flow, $Id1_{ref}$ and $Id1_{ref}$ are the reference d-axis currents for the two VSCs, Id1 and Id2 are the actual d-axis currents.

3.1.2 Reactive power control

The reactive power control loop involves controlling the reactive power flow using the q-axis current components of the two VSCs. The control equation for the reactive power flow is given by:

$$Q_{ref} = Q_{set} - K_p * \left(Iq1_{ref} - Iq1\right) - Kp * \left(Iq2_{ref} - Iq2\right) \tag{4}$$

where Q_{ref} is the desired reactive power flow, Q_{set} is the actual reactive power flow, $Iq1_{ref}$ and $Iq2_{ref}$ are the reference

q-axis currents for the two VSCs, Iq1 and Iq2 are the actual q-axis currents.

3.1.3 Voltage control

The voltage control loop involves controlling the DC voltage of the common DC link to maintain the desired voltage level. The control equation for the DC voltage is given by:

$$Vdc_{ref} = Vdc_{set} - K_i * \left(Vdc - Vdc_{set}\right) \tag{5}$$

where Vdc_{ref} is the reference DC voltage, Vdc_{set} is the desired DC voltage, Vdc is the actual DC voltage, and K_i is the integral gain of the controller. By decoupling the power control into separate control loops, the DPCS can achieve precise control of active and reactive power flow, which can be useful in various power system applications. The mathematical analysis of the strategy helps in designing and tuning the control parameters to achieve the desired control performance.

3.2 Nonlinear and linear dynamic model of 6P-UPFC

3.2.1 Nonlinear dynamic model

The nonlinear dynamic model of the 6P-UPFC includes the VSC, series and shunt converters, and the transmission line. The VSCs are modeled using a voltage-controlled voltage source model, while the series and shunt converters are modeled using current-controlled voltage sources.The dynamic equations for the 6P-UPFC can be expressed as follows:

$$\frac{dVdc}{dt} = -\frac{1}{Ldc} * \left(Vdc - Vdc_{ref}\right) + \frac{1}{Cdc} * \left(Icap - Icap_{ref}\right) \tag{6}$$

$$\frac{dVdq}{dt} = -1/Ldq * Vdq - omega * Vq \tag{7}$$

$$\frac{dIdc}{dt} = -\frac{1}{Rdc} * Idc + \frac{Vdc}{Ldc} - \frac{Vf}{Lf} \tag{8}$$

$$\frac{dIq}{dt} = -\frac{1}{Rf} * Iq - omega * If - \frac{Vq}{Lf} \tag{9}$$

$$\frac{dIf}{dt} = -\frac{1}{Lf} * (If - Iq - Icomp) \tag{10}$$

$$\frac{dIcomp}{dt} = -\frac{1}{Rcomp} * Icomp + \frac{1}{Lcomp} * (If - Icomp) \tag{11}$$

where Vdc and Vdq are the voltage components of the VSC, Icap is the current through the shunt converter, Vdc_{ref} and $Icap_{ref}$ are the reference values for the VSC and shunt converter, respectively, Ldc and Ldq are the VSC inductances, omega is the angular frequency, Vq is the series converter voltage, Rdc is the VSC resistance, Vf is the transmission line voltage, Lf is the transmission line inductance, Rf is the transmission line resistance, If is the transmission line current, *Icomp* is the compensating current, *Rcomp* is the compensating resistance, and *Lcomp* is the compensating inductance.

3.2.2 Linear dynamic model

By linearizing the nonlinear dynamic model of the 6P-UPFC at a nominal operating point, a linear dynamic model of the device was generated. It is possible to write out the linearized model in state-space form as:

$$\frac{dx}{dt} = Ax + Buy = Cx + Du \tag{12}$$

the input vector u, the state vector x, and the result vector y. In addition, D stands for the direct transmission matrix, A for the state matrix, B for the input matrix, C for the output matrix, and so on. The state vector includes the voltages and currents at various points in the 6P-UPFC system. The input vector includes the reference values for the VSC and shunt converter, as well as the fault signal. The output vector includes the measured voltages and currents. The linear dynamic model can be used to design control algorithms for the 6P-UPFC system, such as state feedback control and observer-based control. The nonlinear dynamic model, on the other hand, can be used to analyze the stability and performance of the system under various operating conditions.

3.3 IGWO optimization

In recent years, researchers have focused on enhancing the control strategies of the UPFC to achieve more efficient power management and control. One such strategy is the DPCS, which aims to independently control the active and reactive power flows in the transmission line. By decoupling these power flows, it becomes possible to regulate each component individually, thereby improving the overall power quality and system performance. To further enhance the DPCS, researchers have turned to optimization algorithms for tuning the controller parameters. Among these algorithms, the IGWO algorithm has gained attention due to its effectiveness in solving complex optimization problems. The IGWO algorithm is inspired by the hunting behavior of gray wolves and mimics their social hierarchy to iteratively search for optimal solutions. In this work, an

IGWO-DPCS is proposed to enhance power quality, reduce losses, and improve system stability by optimizing the control parameters.

The IGWO-DPCS divides its control efforts between reactive power control and active power control, enabling precise regulation of voltage and phase angle.In addition to the optimization-based control strategy, a fault isolation technique is introduced to enhance the system's dependability and efficiency. By analyzing voltage and current signals at the UPFC terminals, as well as line impedance, the presence of faults or damaged parts in the transmission line can be detected. Once the fault location is identified, the 6P-UPFC is adjusted to compensate for the predicted impedance of the damaged line, restoring power to the system.The proposed IGWO-DPCS offers several advantages over conventional control strategies. Firstly, the optimization of controller parameters using the IGWO algorithm ensures efficient and precise control of the 6P-UPFC, leading to improved power quality indicators such as power factor and total harmonic distortion. Secondly, the decoupled control approach allows independent regulation of active and reactive power, providing more flexibility and adaptability in power flow management. Lastly, the fault isolation technique enhances system reliability by facilitating quick fault detection and restoration, minimizing downtime, and improving overall system performance.

The mathematical analysis of the 6P-UPFC involves understanding the equations that govern the behavior of the device. The 6P-UPFC is essentially a combination of two VSCs that are connected in series through a common DC link. The VSCs generate two sets of three-phase voltages that can be independently controlled in terms of amplitude, phase, and frequency. Basic 6P-UPFC equations was written in the d-q reference frame, with the d-axis pointing in the direction of the system's positive sequence and the q-axis pointing in the opposite direction. The IGWO block diagram is seen in Fig. 3. Table 1 shows the detailed analysis of various parameters used in IGWO with their initial values, minimum–maximum values. The following is a summary of the algorithm stages for optimizing the DPCS for 6P-UPFC with IGWO:

Step 1 Set the initial values for the IGWO algorithm's parameters, including the maximum number of iterations and the number of wolves and search space borders that are allowed.

Step 2 Do an initialization of the control parameters, which includes determining the proportional and integral gains for the active power, reactive power, and DC voltage control loops.

Step 3 Evaluate the fitness of each wolf by calculating the objective function value using the current control parameters.

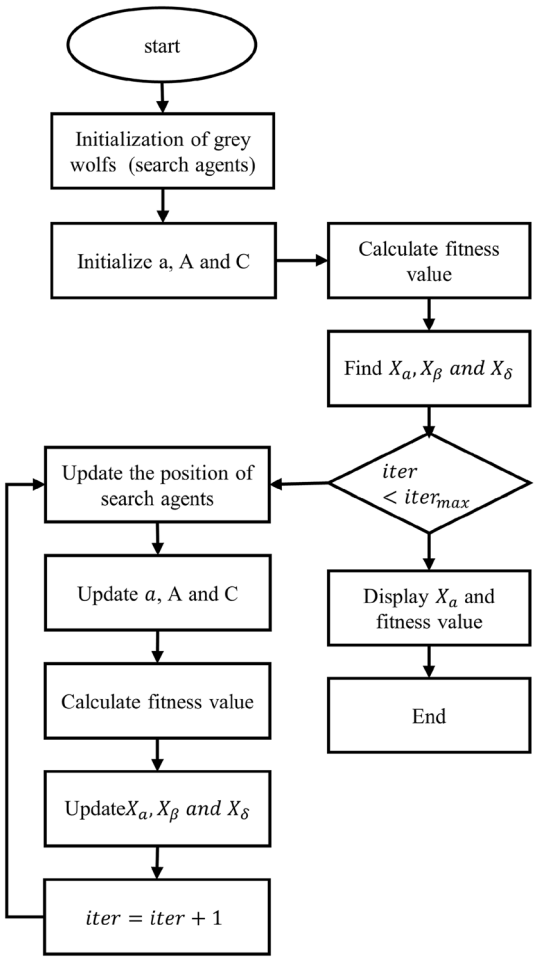

Fig. 3 Proposed IGWO-DPCS block diagram

Step 4 Identify the alpha, beta, and delta wolves with the highest, second highest, and third-highest fitness values, respectively.

Step 5 Update the positions of the alpha, beta, and delta wolves using the following equation:

$$x_{new} = alpha_{pos} - A * \left(beta_{pos} - delta_{pos}\right) \tag{13}$$

where A is a scaling factor and $alpha_{pos}$, $beta_{pos}$, and $delta_{pos}$ are the positions of the alpha, beta, and delta wolves, respectively. The social structure of the IGWO pack is represented by three grey wolves: an alpha, a beta, and a delta. So far, the alpha wolf has been determined to be the best solution, followed by the beta wolf as the next-best choice, and finally the delta wolf as the least-preferred choice.

Step 6 Update the positions of the other wolves using the following equation:

Table 1 Initial values of IGWO algorithm

Parameter	Initial value
Number of grey wolves (N)	50
Maximum number of iterations (MaxIter)	200
Search space boundaries	[− 1.0, 1.0] (for each variable)
Convergence threshold (Epsilon)	0.0001
Grey wolves' positions	[− 5 to 5], Randomly initialized within the search space
Grey wolves' fitness values	[− 10, 10] Randomly assigned initial fitness values
Leader wolf position	[0, 100] Randomly selected from the initial positions
Leader wolf fitness value	[0, 100] Randomly assigned initial fitness value
Exploration and exploitation parameters	[0, 80] Randomly chosen values within specified ranges

$$x_{new} = \frac{\left(alpha_{pos} + beta_{pos}\right)}{2} - A * \left(rand\left(\left(delta_{pos} - beta_{pos}\right)\right) + rand\left(\left(alpha_{pos} - beta_{pos}\right)\right)\right) \tag{14}$$

where *rand*() is a random number generator function.

Step 7 Ensure that the positions of the wolves do not violate any constraints, such as the limits on the control parameters.

Step 8 Evaluate the fitness of each wolf using the updated positions.

Step 9 Identify the new alpha, beta, and delta wolves with the highest, second highest, and third-highest fitness values, respectively.

Step 10 Update the control parameters using the position of the alpha wolf.

Step 11 Check if the stopping criteria have been met, such as the maximum number of iterations or the convergence of the objective function.

Step 12 If the stopping criteria have not been met, repeat steps 3 to 11.

Step 13 Return the optimized control parameters that minimize the objective function.

So, the DPCS for 6P-UPFC can be optimized using the IGWO algorithm by iteratively updating the control parameters based on the fitness values of a population of wolves. The algorithm aims to find the optimal values of the control parameters that minimize the error between the desired and actual values of active and reactive power flow while maintaining the DC voltage at a desired level.

3.3.1 Time complexity analysis of IGWO

The time complexity analysis of the IGWO algorithm can be described in terms of the number of iterations and the computational complexity of each iteration. In the context of time complexity analysis, we usually focus on the dominant factors that contribute the most to the computational cost. The time complexity of initializing the population of grey wolves is typically negligible compared to the overall algorithmic complexity. Therefore, it can be considered to have a constant time complexity of $O(1)$.Evaluating the fitness of each grey wolf involves calculating the objective function value, which typically depends on the problem being solved. The time complexity of fitness evaluation for each grey wolf is determined by the complexity of the objective function. Let's denote the fitness evaluation time complexity for a single grey wolf as $O(f)$, where f represents the complexity of the objective function.

The IGWO algorithm iteratively improves the solutions through a series of iterations. The number of iterations is often determined by the convergence criteria or a maximum allowed number of iterations. Considering the above factors, the overall time complexity of the IGWO algorithm can be approximated as $O(T * N * f)$, where T is the number of iterations, N is the population size (number of grey wolves), and f represents the complexity of the objective function. It's worth noting that the time complexity analysis assumes that the computational cost of each iteration is dominated by the fitness evaluation step. However, the actual time complexity may vary depending on the specific implementation details, problem complexity, and any additional computational steps involved in the algorithm. Additionally, it's important to consider that the time complexity analysis provides an estimate of the algorithm's computational requirements in terms of growth rates. It does not account for factors like parallelization, implementation optimizations, or specific hardware considerations that may impact the actual runtime performance.

3.3.2 Fault location for six-phase lines

In six-phase transmission systems with a 6P-UPFC, fault location can be determined using mathematical analysis. When a fault occurs in a six-phase line, a fault current will flow through the faulted phase(s). The voltage at the fault location will also be affected, resulting in a voltage drop. These changes in current and voltage can be analyzed to determine the location of the fault. If the fault occurs at location x in the transmission line, the fault current and voltage can be expressed as:

$$i_{fault}(x) = K_{fault} * exp(-j * beta * x) \tag{15}$$

$$v_{fault}(x) = V_{source} * exp(-j * gamma * x) \tag{16}$$

where K_{fault} is a constant related to fault current magnitude, beta is the phase constant, V_{source} is the source voltage, and gamma is the constant. The propagation phase constant and propagation constant can be expressed as:

$$beta = sqrt(3) * omega * L/Z \tag{17}$$

$$gamma = sqrt(3) * omega * sqrt(L * C) \tag{18}$$

where omega is the angular frequency, L is the line inductance, C is the line capacitance, and Z is the line impedance. By measuring the fault current and voltage at different points along the transmission line, the fault location can be determined using the following equation:

$$x = (1/beta) * ln\left(\left|\frac{i_{fault}(x1)}{i_{fault}(x2)}\right|\right) \tag{19}$$

where $\times 1$ and $\times 2$ are two points along the transmission line where the fault current and voltage are measured. In practice, this mathematical analysis was complicated by factors such as line loading, non-idealities in the 6P-UPFC, and the presence of multiple faults. However, the basic principles described above can be used to develop fault location algorithms for six-phase transmission systems with 6P-UPFCs.

3.4 Fault isolation technique of 6P-UPFC

If there is an issue with the AC power supply, it will initially be felt by the series transformer. This is unavoidable due to the 6P architecture of UPFCs and the low tolerance of power electronics. When thinking of a source of regulated current, the valve side winding of a series transformer comes to mind, since it too is governed by the line current. Line current controls this current generator. Series transformers link the rapidly growing line current to the series converter in the case of power outages or other interruptions on the AC power system. With this, the converter has a better chance of continuing to operate normally. The 6P-UPFC project in western Nanjing, which uses the 220 kV grid, was the pioneer in the usage of the rapid bypass technology. This was done for safety reasons regarding the equipment. This technology is the primary means by which the 6P-UPFC project in China addresses the problems of fault isolation and insulation design for the series transformer. The schematic for an isolated circuit with bypass breakers and a series connection is shown in Fig. 4. Each series transformer is equipped

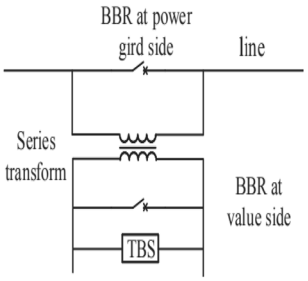

Fig. 4 Structure of isolation technique on series connect unit

with a thyristor bypass switch (TBS) on the grid side and a buck–boost rectifier (BBR) on the valve side.

Every series transformer also has a BBR placed on the valve side. In the case of a malfunction, TBS and BBR may reroute the current from the series transformer winding to the parallel converter. The overall layout of the isolation technique as it is applied to the series-connected unit. If there is an issue with either the AC power grid or the 6P-UPFC, its operation will be compromised. In the case of a malfunction, the protective mechanism of the 6P-UPFC quickly shuts off the offending converter, activates the TBS of 6P-UPFCs to isolate the series connect unit, and then closes the BBR to provide a route for the fault current instead of the TBS. The purpose of this strategy is to prevent the 6P-UPFC from using the rapid bypass function of TBS, which enables fault isolation to take place in as little as 40 ms and BBR closure on both sides of a series transformer to take place in the same amount of time (switching closing time is include). Isolating the series connect unit, shutting off the power gird side switch of the shunt transformer, and isolating the shunt converter are the three steps that make up the fault shutdown procedure for the 6P-UPFC system. The 6P-UPFC system has been successfully disconnected from the public power grid.

The circuit of the 6P-UPFC includes series and shunt converters, a VSC, BBR, and a transmission line. The VSCs are used to regulate the voltage and current of the transmission line, while the series and shunt converters are used to provide series and shunt compensation, respectively. The BBR are used to isolate the faulty section of the transmission line. The fault isolation technique involves detecting a fault on the transmission line, isolating the faulty section using the TBS, and then compensating for the fault using the 6P-UPFC. By comparing the voltage and current flow in the transmission line before and after a problem occurs, we may draw conclusions about the fault isolation method. As was said in a previous comment, the voltage and current will be impacted when a defect develops on the transmission line, and the problem's location was detected using mathematical analysis. The BBR are used to cut off power to the bad segment of the transmission line after the problem has been

located. The 6P-UPFC then adjusts the voltage and current in the transmission line through the VSCs and the series and shunt converters to correct for the problem. The fault isolation technique's control method may also be examined. The 6P-UPFC is used to modify the voltage and current in the transmission line once the fault has been detected and its position calculated. The TBS is then opened to isolate the problematic portion. A state-space model was used to represent the control strategy; in this model, the voltage and current at various nodes in the system serve as state variables, and the reference values for the VSC and series and shunt converters serve as control inputs. The control strategy can also be optimized using IGWO techniques such as optimization algorithms, as described in a previous response.

4 Results and discussion

This section detailed the simulation analysis and implementation specifics for the suggested 6P-UPFC method. The proposed model was built with the help of the MATLAB/SIMULINK software suite. The waveforms of the simulated current, voltage, and power are evaluated to ensure the system is operating as intended. The subsequent improvement in power quality is measured by THD, FST, and power factor. Figure 5 shows the simulation model of 6P-UPFC system. Figure 6 shows the series controller for 6P-UPFC with IGWO function. When a series converter is used to provide series compensation in a transmission line, a series controller is required to regulate the voltage and current flowing through it.

Figure 7 shows the shunt controller for 6P-UPFC with IGWO function. The shunt controller regulates the voltage and current of the shunt converter, which is used to effect shunt compensation in the transmission line. A state-space model was used to characterize both series and shunt controllers, with the voltage and current in the series and shunt converters serving as state variables and the reference values serving as control inputs. In this case, the IGWO algorithm was used to enhance the power quality of the system and reduce losses in the transmission line by modifying the voltage and current reference values

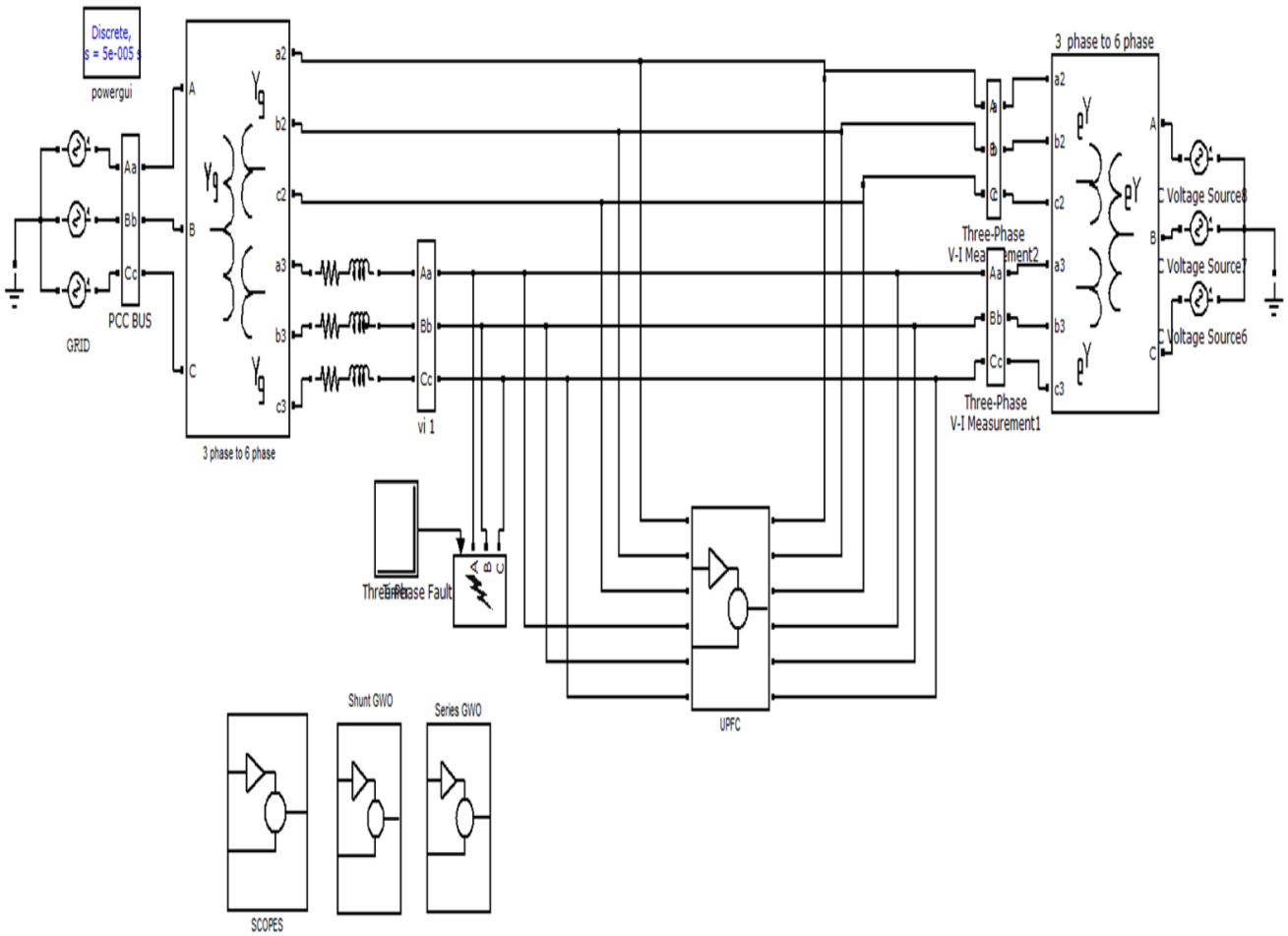

Fig. 5 Simulation model of 6P-UPFC with IGWO

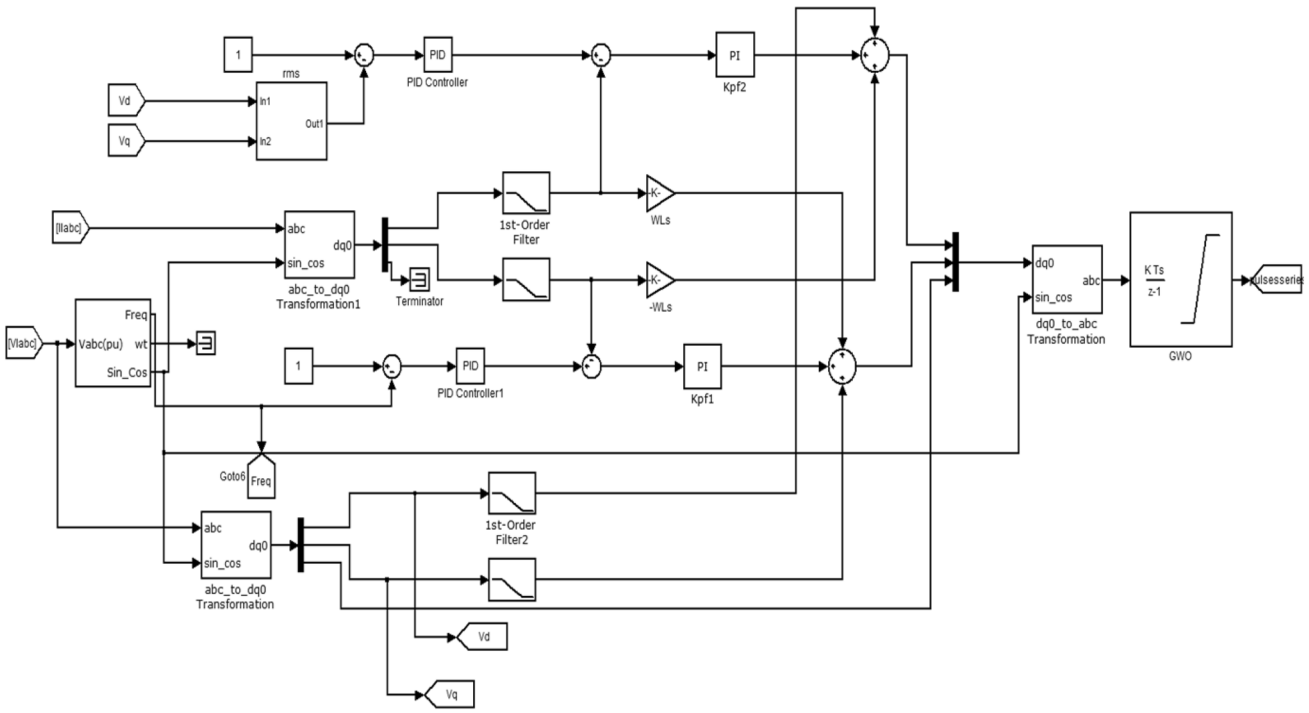

Fig. 6 Series controller for 6P-UPFC with IGWO function

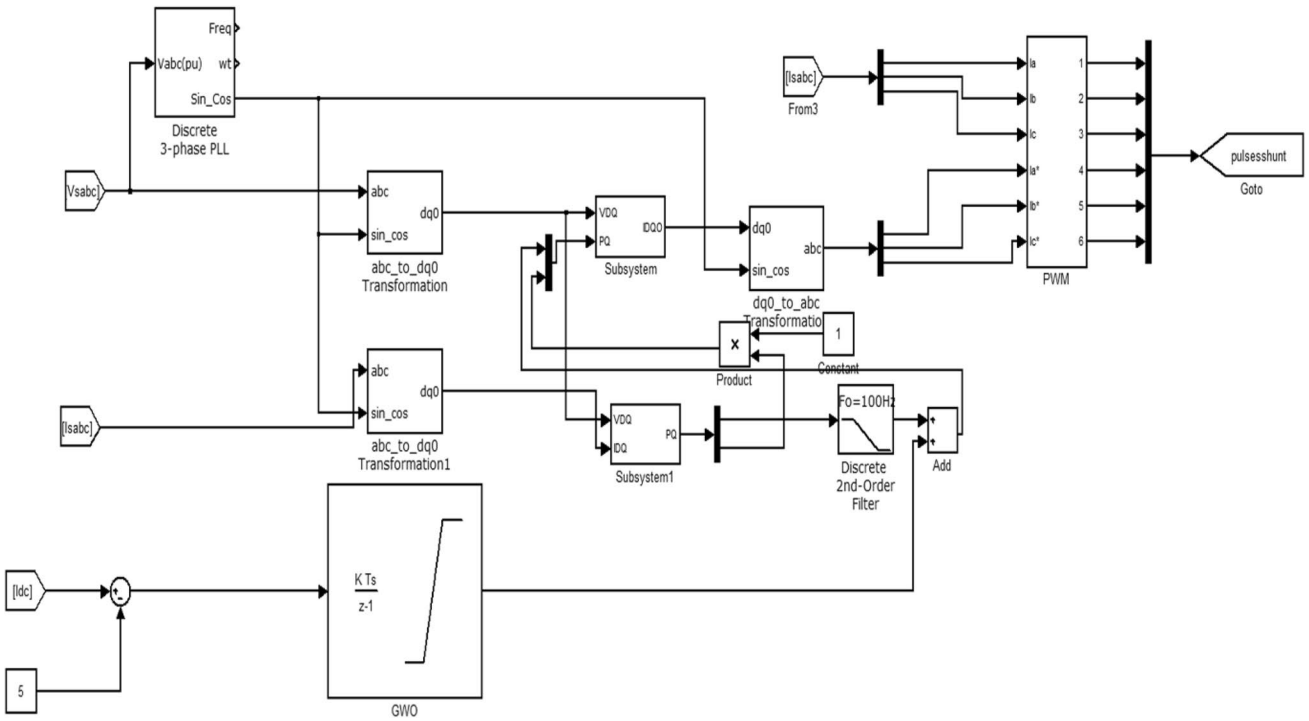

Fig. 7 Shunt controller for 6P-UPFC with IGWO function

utilized by the series and shunt controllers. Optimizing a system entails repeatedly adjusting the voltage and current baselines considering the fitness function, a measure of system performance. Transmission line power loss and voltage and current deviations from ideal values contribute equally to the fitness function. The IGWO algorithm then looks for the minimum-fitness-function voltage and current reference values.

4.1 Simulation results

Figure 8 shows the parameter space, objective space of IGWO for series & shunt converters. The parameter space in IGWO typically includes the design variables that define the problem being optimized. Those are control variables related to the converter topology (e.g., number of switching stages, type of switch used, etc.). These variables can vary widely depending on the problem domain. The objective space in IGWO typically includes the performance metrics or criteria that the optimizer is trying to optimize. Figure 9 shows the three phase voltages such as LLL fault voltage, IGWO based 6P-UPFC compensated voltage, and load voltage. LLL (Line-to-Line-to-Line) fault voltage is the voltage that occurs when a three-phase fault occurs in a power system. The voltage is typically very high and can cause significant damage to equipment if not properly controlled. The IGWO algorithm can be used in conjunction with a 6P-UPFC to compensate for the LLL fault voltage and maintain stable load voltage. LLL fault voltage is the voltage that occurs when a three-phase fault occurs in a power system. The voltage is typically very high and can cause significant damage to equipment if not properly controlled. The IGWO algorithm can be used in conjunction with a 6P-UPFC to compensate for the LLL fault voltage and maintain stable load voltage.

Figure 10 shows the three phase voltages such as LG fault voltage, IGWO based 6P-UPFC compensated voltage, load voltage. LG (Line-to-Ground) fault voltage is a type of fault that can occur in a power system where one of the three-phase lines becomes grounded. This can cause an imbalance in the system and result in a high voltage at the fault location, which can damage equipment and disrupt power supply. The IGWO algorithm can be used in conjunction with a 6P-UPFC to compensate for the LG fault voltage and maintain stable load voltage.

Figure 11 shows the six phase voltages after 6P-UPFC-IGWO based compensation. The exact values of the voltages will depend on the specific control parameters optimized by the IGWO algorithm, as well as the characteristics of the power system being controlled. To correct power grid inequalities and disruptions, phase shifts in voltages were used. If the voltages are equalized throughout all six phases, the

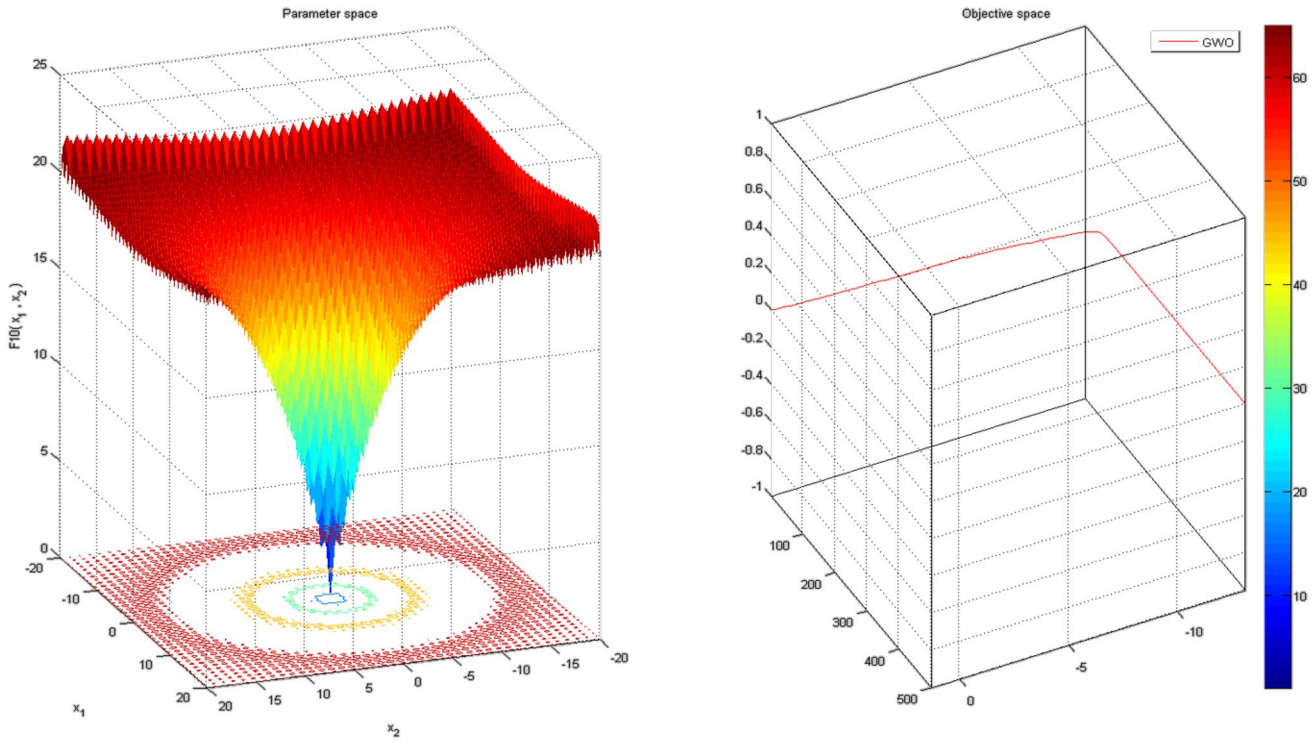

Fig. 8 Parameter space, objective space of IGWO for series & shunt converters

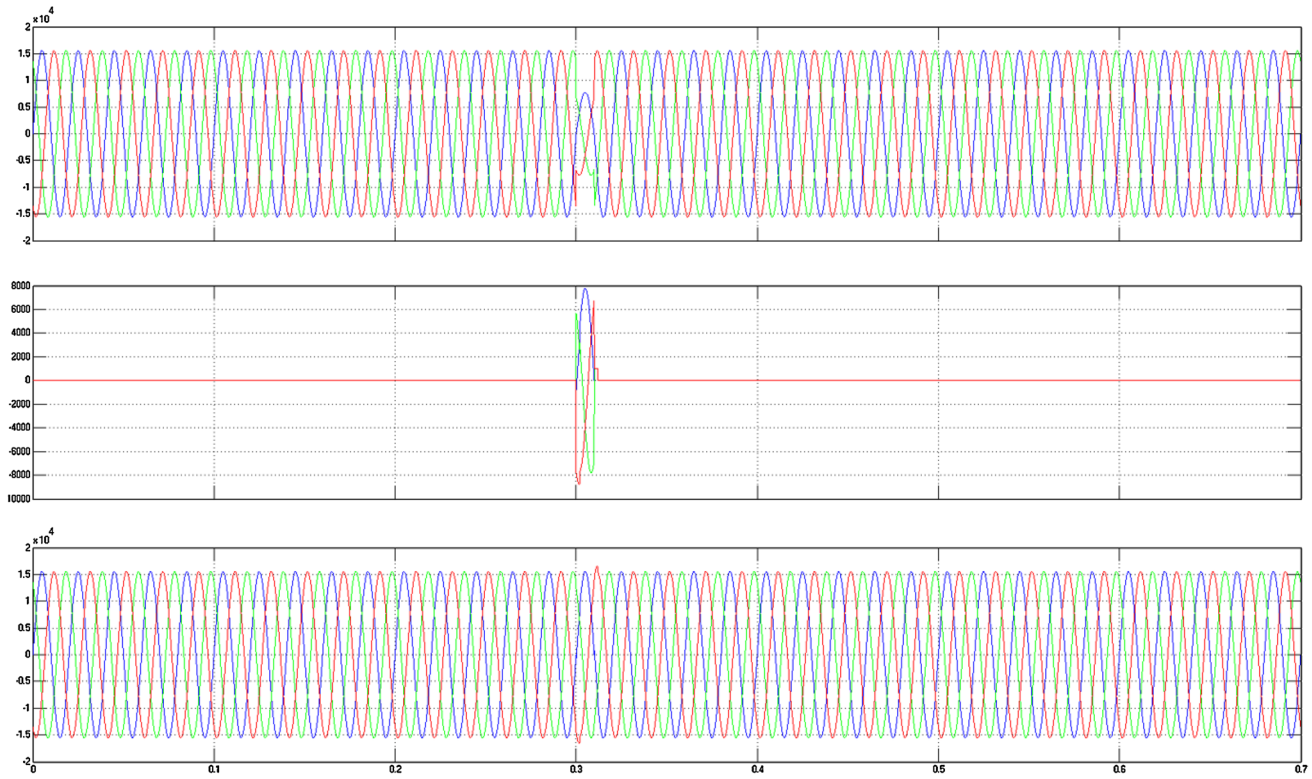

Fig. 9 Three phase voltages (LLL fault voltage, IGWO based 6P-UPFC compensated voltage, load voltage)

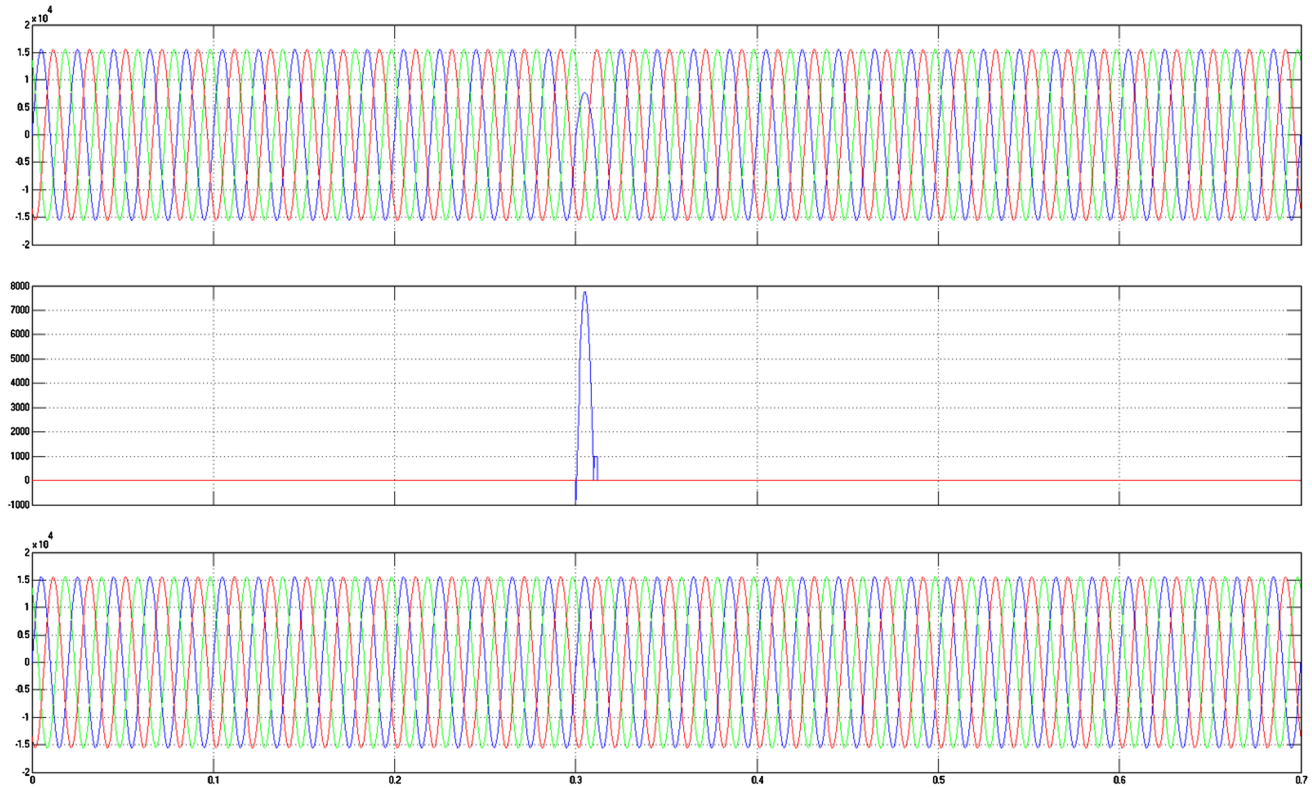

Fig. 10 Three phase voltages (LG fault voltage, IGWO based 6P-UPFC compensated voltage, load voltage)

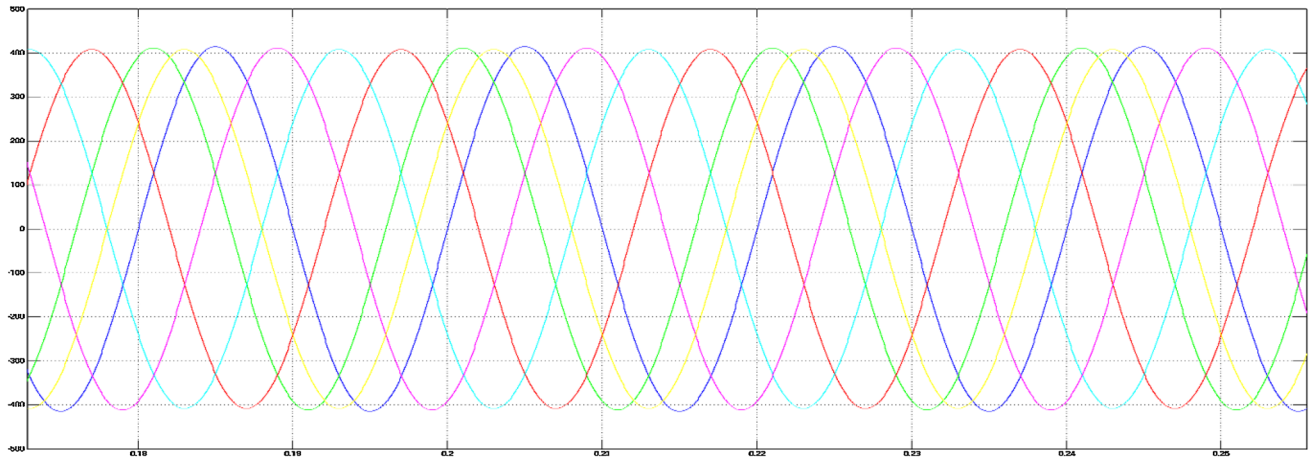

Fig. 11 Six phase voltages after 6P-UPFC-IGWO based compensation

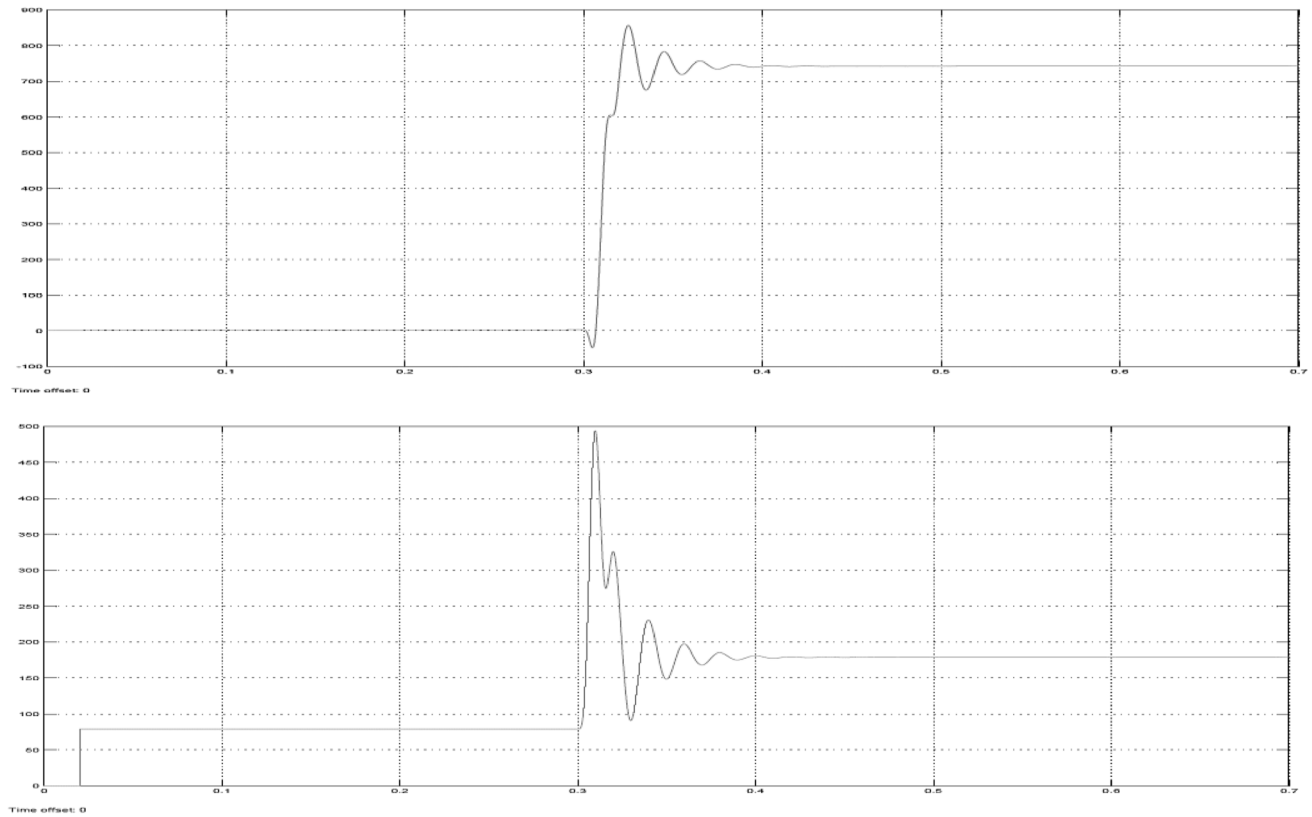

Fig. 12 Active & Reactive power of without 6P-UPFC-IGWO based compensation

system is more likely to run smoothly and reliably. Improving power quality is possible by reducing or eliminating harmonic distortions and other undesired characteristics of voltage waveforms.

In Fig. 12 shown that the active and reactive power of the without 6P-UPFC compensation. In Fig. 13, we can see the active and reactive power of the 6P-UPFC when it is under load. The 6P-UPFC permits control of both active and reactive power flows at the load. With the 6P-UPFC, the phase and amplitude of the voltage injection was independently adjusted to control the actual and reactive power flows. As a result, the 6P-control UPFC's strategy and the power demand of the load will determine the active and reactive power at the connected load.Fig. 14 shows the

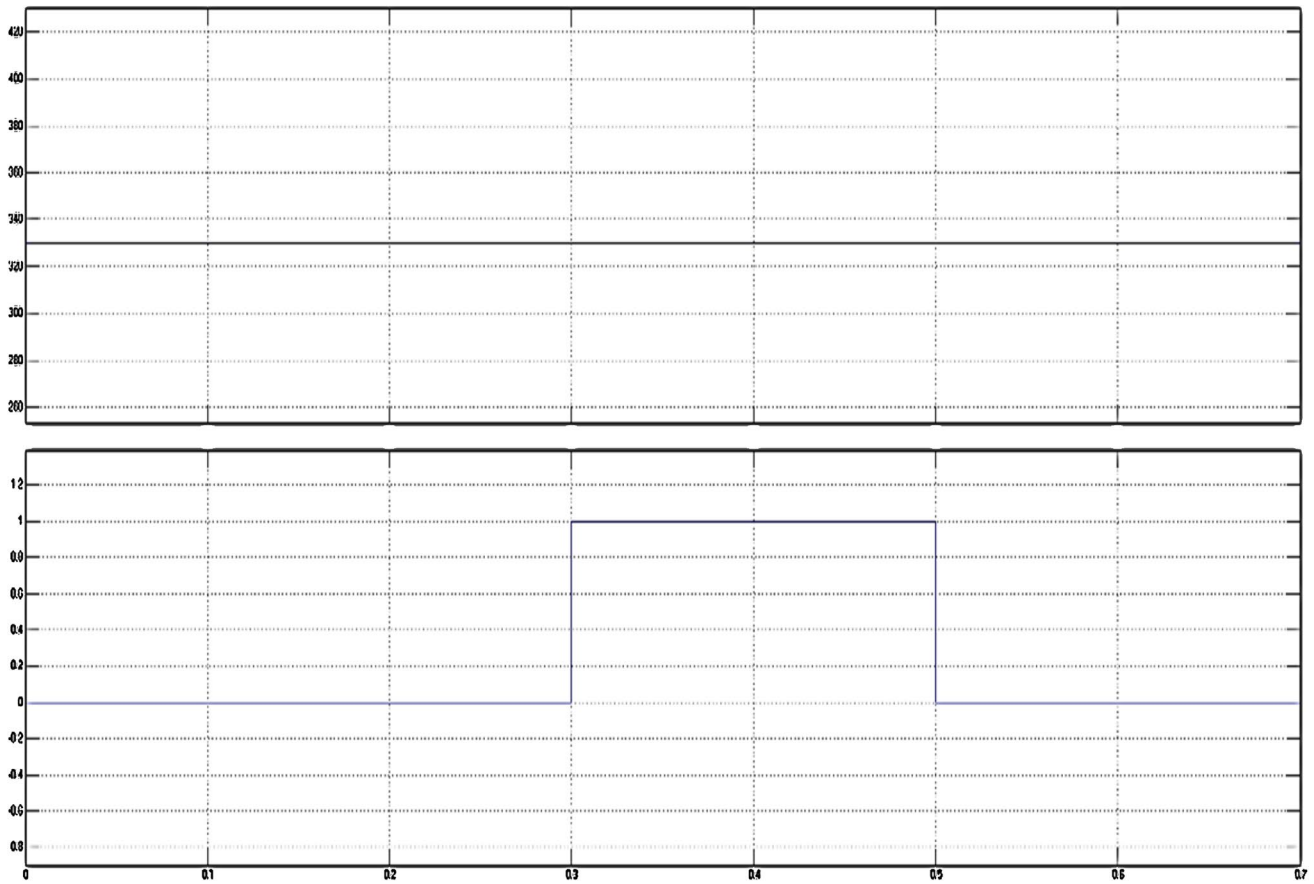

Fig. 13 Active & Reactive power at the load

Root Mean Square (RMS) voltage before and after compensation. The RMS voltage is a measure of the effective voltage level of an AC waveform, and it is calculated as the square root of the mean of the squared instantaneous voltage values over a cycle. Before compensation with a 6P-UPFC, the RMS voltage at a load was affected by voltage drop and other factors in the transmission and distribution system. The voltage level was below or above the desired level, which can affect the performance and efficiency of the load. After compensation with a 6P-UPFC, the RMS voltage at the load can be adjusted and regulated to the desired level. The 6P-UPFC can inject or absorb reactive power into the system to compensate for voltage drop and other factors and regulate the voltage level at the load. The degree of improvement in the RMS voltage level after compensation with a 6P-UPFC will depend on the control strategy used by the 6P-UPFC, the system parameters, and the load demand. In general, the 6P-UPFC can help improve the power quality at the load and ensure that the voltage level is within the desired range.

Compensation's effect on the power factor is seen in Fig. 15. A 6P-UPFC may adjust for the reactive power requirement of the load, and then inject or absorb reactive power to enhance the power factor at the load. By controlling the voltage's phase and amplitude, the 6P-UPFC can keep the power factor where it needs to be. To what extent a load makes use of the available electrical power is represented by a metric called the power factor. Simply put, it is the ratio of the load's actual power consumption (in watts) to its perceived power consumption (in volt-amperes). If the power factor is 0.98, the load is making efficient use of the supplied electricity.

Compensation results for the THD are shown in Fig. 16. The THD quantifies the degree to which voltage or current waveforms are distorted. The THD was reduced by tailoring the design of the series and shunt controllers. This can be achieved by using control algorithms that can generate waveforms that are as close to sinusoidal as possible. The IGWO algorithm can be used to optimize the control algorithms to reduce THD and improve the power quality of the system.

Table 2 compares the performance comparison of various controllers in 6P-UPGC environment. The FST is the time it takes for the protection system to detect and isolate a fault in the transmission line. To reduce the FST, THD, the series

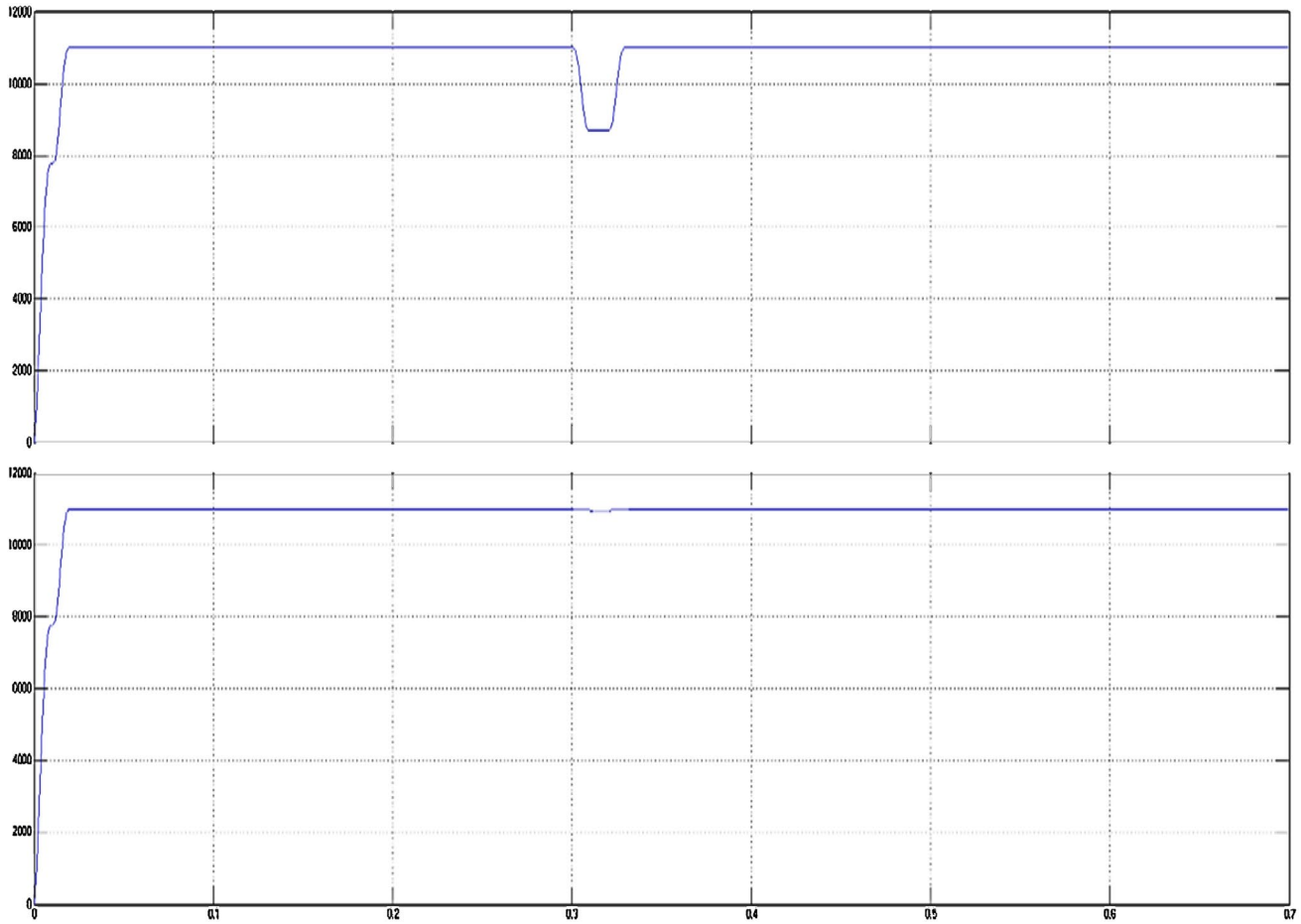

Fig. 14 RMS voltage before and after compensation

and shunt controllers can be designed to respond quickly to changes in the system. This can be achieved by using fast-acting control algorithms that can detect faults in real-time and quickly adjust the voltage and current in the system to compensate for the fault. The IGWO algorithm can be used to optimize the control algorithms to improve power quality and reduce the FST, THD in comparison with existing DSTATCOM, existing 6P-UPFC-MBO methods.

Table 3 compares the voltage-Current Performance comparison. Voltage Regulation: The information provided does not specify the values for voltage regulation for the existing DSTATCOM and existing 6P-UPFC-MBO methods. Both the existing DSTATCOM and existing 6P-UPFC-MBO methods provide reactive power compensation. Similarly, the proposed DPCS 6P-UPFC-IGWO method also includes reactive power compensation. While the existing DSTATCOM does not offer harmonic mitigation, the existing 6P-UPFC-MBO method incorporates harmonic mitigation techniques. Similarly, the proposed DPCS 6P-UPFC-IGWO method also includes harmonic mitigation capabilities. The existing DSTATCOM does not have voltage sag compensation features. In contrast, both the existing 6P-UPFC-MBO and proposed DPCS 6P-UPFC-IGWO methods provide voltage sag compensation. Like voltage sag compensation, the existing DSTATCOM does not provide voltage swell compensation. However, both the existing 6P-UPFC-MBO and proposed DPCS 6P-UPFC-IGWO methods incorporate voltage swell compensation capabilities. The information does not explicitly mention the dynamic voltage stability for the existing DSTATCOM method. However, the existing 6P-UPFC-MBO method improves dynamic voltage stability. Similarly, the proposed DPCS 6P-UPFC-IGWO method also enhances dynamic voltage stability compared to the existing methods.

4.2 Discussions

Determining the cost-effectiveness of a 6P-UPFC involves considering various factors beyond the cost of the FACTS devices themselves. While FACTS devices are generally considered costly, the cost-effectiveness of a 6P-UPFC can be evaluated by examining its potential benefits and comparing them to the overall system costs. The 6P-UPFC can offer

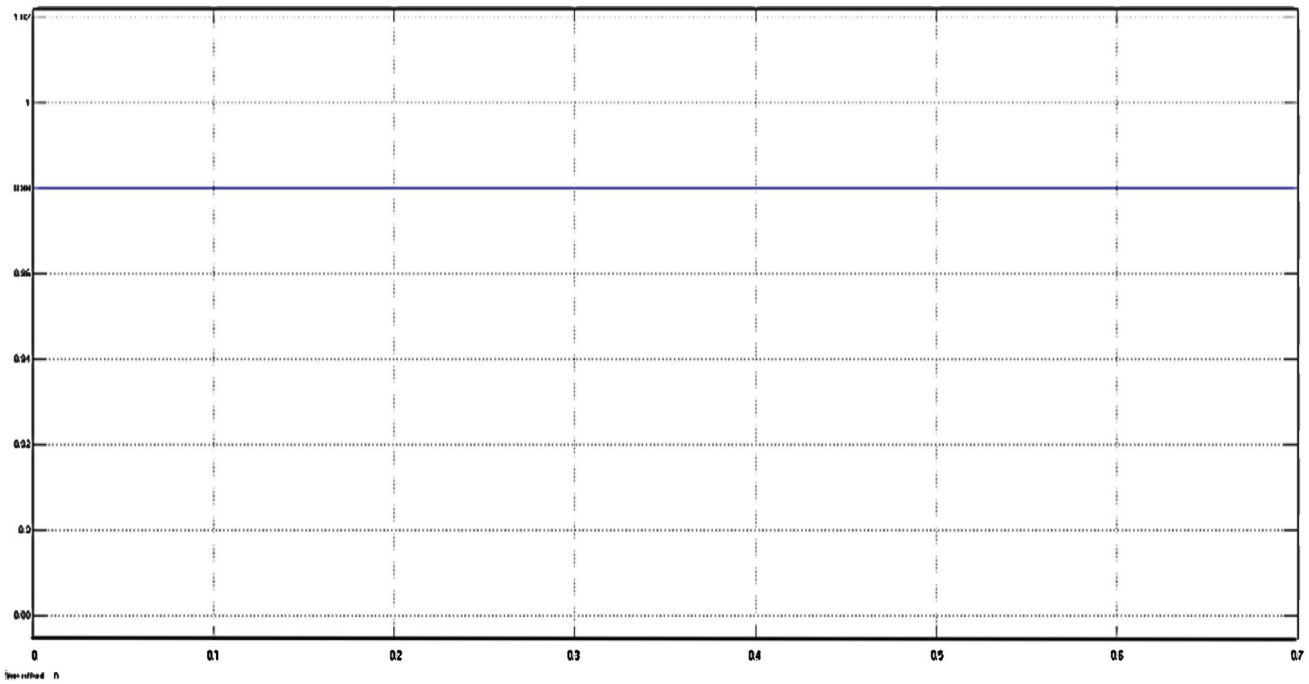

Fig. 15 Power factor after compensation

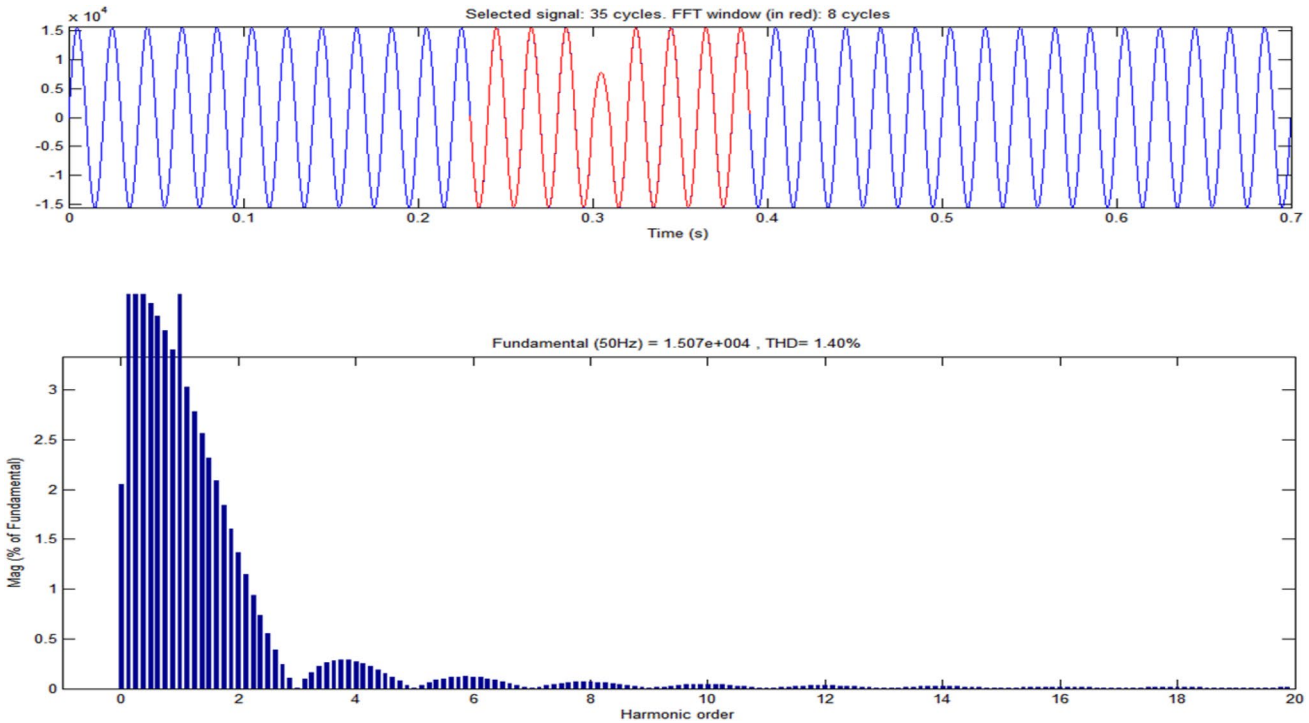

Fig. 16 THD after compensation

enhanced power flow control, voltage stability, and transient stability in the power system. By mitigating power quality issues, improving system reliability, and reducing losses, it can lead to operational cost savings and increased efficiency.

While the proposed strategy utilizes the IGWO method for parameter optimization, future research could explore other advanced optimization techniques or hybrid approaches to further enhance the control strategy's performance.

Table 2 Performance comparison

Parameters	Existing DSTATCOM	Existing 6P-UPFC-MBO	Proposed DPCS 6P-UPFC-IGWO
FST	0.15 s (0.25–0.4)	0.1 s (0.3–0.4)	0.01 s (0.3–0.31)
Power factor	0.6	0.78	0.98
THD	20%	10.33%	1.40%

Table 3 Voltage-current performance comparison

Parameters	Existing DSTAT-COM	Existing 6P-UPFC-MBO	Proposed DPCS 6P-UPFC-IGWO
Voltage regulation	–	–	Improved
Reactive power compensation	Yes	Yes	Yes
Harmonic mitigation	No	Yes	Yes
Voltage sag compensation	No	Yes	Yes
Voltage swell compensation	No	Yes	Yes
Dynamic voltage stability	–	Improved	Improved

Comparisons with alternative optimization algorithms could help identify the most suitable optimization approach for the 6P-UPFC-DPCS.The control strategy could be extended to incorporate communication systems for improved coordination and control of multiple UPFC devices in a power network. Future studies could investigate the impact of communication delays and develop communication-assisted control algorithms to enhance the overall system performance. The study focuses on a specific 6P-UPFC configuration, but it would be worthwhile to explore the scalability of the proposed control strategy for different UPFC configurations. Investigating the applicability and effectiveness of the strategy in systems with different numbers of phases or varying UPFC topologies would provide valuable insights.

So, to overcome these problems, further exploration and development of advanced control strategies can be investigated to enhance the performance of the UPFC. This could involve the use of intelligent control techniques such as neural networks, ANFIS, MPC to optimize power flow control, voltage stability, and harmonics mitigation. With the increasing integration of renewable energy sources into the power grid, there is a need to investigate the application of the six-phase UPFC in renewable energy systems. Future research could focus on optimizing the control strategy to accommodate the dynamic characteristics and variability of renewable energy sources, such as solar and wind power. The proposed UPFC design and control strategy can be further evaluated for large-scale implementation in real-world power systems. Future studies could involve conducting field trials or real-time simulations to assess the practicality, scalability, and economic viability of the proposed solution.

5 Conclusion

This study suggests a DPCS for use in a 6P-UPFC as a means of improving power quality in conjunction with the IGWO algorithm. According to the 6P-UPFC-DPCS, the control task was broken down into two distinct subtasks: reactive power control and active power control. As the UPFC regulates both the active and reactive power flows, it may independently adjust both the broadcast line voltage and the phase angle. There has been a presentation of a fault isolation strategy to further improve the system's performance and resilience. The problematic section of the transmission line was located, and the system optimized with the use of this technology. To provide the groundwork for fault identification, the line impedance and voltage and current signals at the UPFC's terminals are examined. When the faulty part has been located, an estimate of the faulted line's impedance is made, and then the settings of the 6P-UPFC are changed such that power may once again flow through the system. Then, the virtual impedance is utilized to regulate the system's voltage and current, making it the cornerstone of the coordination method. The value of the virtual impedance is changed to accomplish this. Parameters of the controllers are optimized using the IGWO technique. They include the voltage phase angle and magnitude of the inverter, as well as the proportionate and integral gains of the PI controllers. Many offline tests have been performed to determine the accuracy of this method. The complexity of the many forms of faults that might occur is examined, high path fault resistances (0–100), including fault locations (0–100%), and fault initiation angles (0 and 90°) (AG, BG, CD, DG, EG, FG, and

ABCG). The simulation results show that the proposed 6P-UPFC-DPCS might reduce the FST to 0.01 s, boost the power factor to 0.98, and lower the THD to 1.40%. The simulation results indicate that it is possible to identify and diagnose single-phase-to-ground problems in less than one cycle. The method is insensitive to variations in fault characteristics such as fault location, fault resistance and fault inception angle.

Acknowledgements Not applicable.

Author contributions SN contributed to technical and conceptual content, architectural design. RB contributed to guidance and TS contributed to counseling on the writing of the paper.

Funding No funding received by any government or private concern.

Data availability Data sharing not applicable to this article as no datasets were generated or analyzed during the current study.

Declarations

Conflict of interest The authors declare that they have no competing interests.

Human participants and/or animals This article does not contain any studies involving animals performed by any of the authors.

Informed consent Not applicable.

References

Abasi M et al (2020) Accurate simulation and modeling of the control system and the power electronics of a 72-pulse VSC-based generalized unified power flow controller (GUPFC). Electr Eng 102(4):1795–1819. https://doi.org/10.1007/s00202-020-00993-w

Albatsh FM et al (2017) Fuzzy-logic-based UPFC and laboratory prototype validation for dynamic power flow control in transmission lines. IEEE Trans Industr Electron 64(12):9538–9548

Biswal S, Biswal M, Malik OP (2018) Hilbert Huang transform based online differential relay algorithm for a shunt-compensated transmission line. IEEE Trans Power Deliv 33(6):2803–2811

Bone G, Pantoš M, Mihalič R (2018) Newtonian steady state modeling of FACTS devices using unaltered power-flow routines. IEEE Trans Power Syst 34(2):1216–1226

Chen B et al (2018) Research on an improved hybrid unified power flow controller. IEEE Trans Ind Appl 54(6):5649–5660

Elamari K, Lopes LAC (2019) Implementation and experimental verification of a novel control strategy for a UPFC-based interphase power controller. IEEE Trans Power Deliv 34(6):2079–2088

Elsaharty MA et al (2018) Three-phase custom power active transformer for power flow control applications. IEEE Trans Power Electron 34(3):2206–2219

Fang Y et al (2018) Impact of inverter-interfaced renewable energy generators on distance protection and an improved scheme. IEEE Trans Ind Electron 66(9):7078–7088

Hamdan I, Ibrahim AMA, Noureldeen O (2020) Modified STATCOM control strategy for fault ride-through capability enhancement of grid-connected PV/wind hybrid power system during voltage sag. SN Appl Sci 2(4):362–364

Haque MM et al (2020) A UPFC for voltage regulation in LV distribution feeders with a DC-link ripple voltage suppression technique. IEEE Trans Ind Appl 56(6):6857–6870

Hassan LH et al (2013) Application of genetic algorithm in optimization of unified power flow controller parameters and its location in the power system network. Int J Electr Power Energy Syst 46:89–97. https://doi.org/10.1016/j.ijepes.2012.10.011

Kamel S et al (2015) Advanced modeling of center-node unified power flow controller in NR load flow algorithm. Electr Power Syst Res 121:176–182. https://doi.org/10.1016/j.epsr.2014.12.013

Kumar AN, Chakravarthy M (2018) Fuzzy inference system based distance estimation approach for multi location and transforming phase to ground faults in six phase transmission line. Int J Comput Intell Syst 11(1):757–769

Mahajan S, Pandit AK (2021) Hybrid method to supervise feature selection using signal processing and complex algebra techniques. Multimed Tools Appl 81(2):1–22. https://doi.org/10.1007/s11042-020-09803-x

Mahajan S, Pandit AK (2022) Image segmentation and optimization techniques: a short overview. Medicon Eng Themes 2(2):47–49

Mahajan S et al (2022a) Image segmentation approach based on adaptive flower pollination algorithm and type II fuzzy entropy. Multimed Tools Appl 81(13):1–23. https://doi.org/10.1007/s11042-022-13227-1

Mahajan S et al (2022b) Hybrid Aquila optimizer with arithmetic optimization algorithm for global optimization tasks. Soft Comput 26(10):4863–4881. https://doi.org/10.1007/s00500-022-06771-7

Mahajan S et al (2022c) Fusion of modern meta-heuristic optimization methods using arithmetic optimization algorithm for global optimization tasks. Soft Comput 26(14):6749–6763. https://doi.org/10.1007/s00500-022-08040-2

Mahajan S, Abualigah L, Pandit AK (2022d) Hybrid arithmetic optimization algorithm with hunger games search for global optimization. Multimed Tools Appl 81(20):28755–28778. https://doi.org/10.1007/s11042-022-14180-2

Makvandi H et al (2021) A new optimal design of ACD-based UPFC supplementary controller for interconnected power systems. Measurement 182:109670. https://doi.org/10.1016/j.measurement.2021.109670

Miotto EL et al (2018) Coordinated tuning of the parameters of PSS and POD controllers using bioinspired algorithms. IEEE Trans Ind Appl 54(4):3845–3857

Monteiro J et al (2014) Linear and sliding-mode control design for matrix converter-based unified power flow controllers. IEEE Trans Power Electron 29(7):3357–3367. https://doi.org/10.1109/TPEL.2013.2282256

Nouri T et al (2018) An interleaved high step-up converter with coupled inductor and built-in transformer voltage multiplier cell techniques. IEEE Trans Ind Electron 66(3):1894–1905

Ong S-Q et al (2022) Comparison of pre-trained and convolutional neural networks for classification of jackfruit artocarpus integer and artocarpus heterophyllus. In: Classification applications with deep learning and machine learning technologies, Springer, pp 129–141. https://doi.org/10.1007/978-3-030-99628-1_11

Parvathy S, Sindhu Thampatty KC (2015) Dynamic modeling and control of UPFC for power flow control. Proc Technol 21:581–588. https://doi.org/10.1016/j.protcy.2015.10.061

Parvathy S et al (2020) Design and implementation of partial feedback linearization controller for unified power flow controller. Electr

Power Syst Res 187:106438. https://doi.org/10.1016/j.epsr.2020.106438
Qi Y et al (2018) Small signal frequency-domain model of a LCC-HVDC converter based on an infinite series-converter approach. IEEE Trans Power Deliv 34(1):95–106
Sarkar MNI, Meegahapola LG, Datta M (2018) Reactive power management in renewable rich power grids: a review of grid-codes, renewable generators, support devices, control strategies and optimization algorithms. IEEE Access 6:41458–41489
Sengolrajan T, Kalaivani C, Ashok J, Manikandan A (2023) A novel design of 9 level cascade multi-level inverter for decoupled double synchronous reference frame in state delay controller. J Eng Res. https://doi.org/10.1016/j.jer.2023.100106
Sengupta S, Kumar A, Tiwari S (2018) Transient stability enhancement of a hybrid Wind-PV farm incorporating a STATCOM. In: 2018b 3rd IEEE international conference on recent trends in electronics, information and communication technology (RTEICT), pp 1574–1580. https://doi.org/10.1109/RTEICT42901.2018.9012385
Sharma S et al (2022) Image-based automatic segmentation of leaf using clustering algorithm. Int J Nanotechnol 19(6–11):539–553. https://doi.org/10.1504/IJNT.2022.119456
Shotorbani AM et al (2018) A decentralized multiloop scheme for robust control of a power flow controller with two shunt modular multilevel converters. IEEE Trans Ind Inform 14(10):4309–4321
Singh R et al (2022) Impact of quarantine on fractional order dynamical model of Covid-19. Comput Biol Med 151:106266. https://doi.org/10.1016/j.compbiomed.2022.106266
Smith J (2023) Advancements in renewable energy technologies: a comprehensive review. Renew Energy Rev 150:111234
Taheri MM et al (2018) High-speed decision tree based series-compensated transmission lines protection using differential phase angle of superimposed current. IEEE Trans Power Deliv 33(6):3130–3138
Tamimi B, Cañizares CA (2018) Modeling and application of hybrid power flow controller in distribution systems. IEEE Trans Power Deliv 33(6):2673–2682
Tiwari S, Kumar A, Sengupta S (2018) Voltage stability analysis with a novel hybrid controller using shunt and series combination of FACTS device. In: 2018a 3rd IEEE international conference on recent trends in electronics, information an communication technology (RTEICT), pp 885–890. https://doi.org/10.1109/RTEICT42901.2018.9012250
Tiwari S, Kumar A (2023) Advances and bibliographic analysis of particle swarm optimization applications in electrical power system: concepts and variants. Evol Intel 16(1):23–47. https://doi.org/10.1007/s12065-021-00661-3
Wai R-J, Yang Y (2019) Design of backstepping direct power control for three-phase PWM rectifier. IEEE Trans Ind Appl 55(3):3160–3173. https://doi.org/10.1109/TIA.2019.2893832
Wang X (2022) Control and modulation of a single-phase AC/DC converter with smooth bidirectional mode switching and symmetrical decoupling voltage compensation. IEEE Trans Power Electron 37(4):3836–3853. https://doi.org/10.1109/TPEL.2021.3120006
Yadav S, Tiwari S, Kumar A (2020) Transient stability analysis of multi-machine power system with hybrid power flow controller. In: 2020 international conference on power, instrumentation, control and computing (PICC), pp 1–6. https://doi.org/10.1109/PICC51425.2020.9362390
Yan S et al (2021) A review on direct power control of pulsewidth modulation converters. IEEE Trans Power Electron 36(10):11984–12007. https://doi.org/10.1109/TPEL.2021.3070548
Yang J et al (2019) System-level control strategy of UPFC in regional power grids. In: 2019 IEEE PES Asia-pacific power and energy engineering conference (APPEEC), pp 1–5. https://doi.org/10.1109/APPEEC45492.2019.8994424
Yu J et al. (2021) Research on power flow control strategy of weak grid based on series-shunt combined converter. In: 2021 IEEE sustainable power and energy conference (iSPEC), pp 2892-2900. https://doi.org/10.1109/iSPEC53008.2021.9736104
Yuan J et al (2022) A novel multiline fast electromagnetic unified power flow controller topology for distribution network. IEEE Trans Ind Appl 58(3):3238–3249. https://doi.org/10.1109/TIA.2022.3158373
Zhang Y et al (2018) Single-stage AC–AC converter with controllable phase and amplitude. IEEE Trans Power Electron 34(7):6991–7000
Zhu X et al (2018) Subsynchronous resonance and its mitigation for power system with unified power flow controller. J Mod Power Syst Clean Energy 6(1):181–189